Supporting Information for:

Technical Note

Electrochemical wet-cell fabrication for *in situ* soft-X ray hyperspectral imaging of real-life ORR electrocatalysts

Benedetto Bozzini*[1], Alessandro Alleva[1], Maria Eugenia Fortes Brollo[2,3], Regina Ciancio[3,2], Simone Dal Zilio[2], George Kourousias[4], Francesco Nespoli[1], Paolo Ronchese[3,2] and Alessandra Gianoncelli[4]

[1]Department of Energy, Politecnico di Milano, via Lambruschini 4, 20156 Milano, Italy
[2]CNR-IOM, Area Science Park Basovizza, SS 14 km 163.5 - 34139 Trieste, Italy
[3]Area Science Park, Padriciano 99, 34139 Trieste, Italy
[4]Elettra - Sincrotrone Trieste S.C.p.A. S.S, 14, km 163.5 in Area Science Park, 34149 Trieste-Basovizza, Italy

*corresponding author: benedetto.bozzini@polimi.it

S1. Literature overview on *ex situ* spectral STXM studies of model electrocatalyst materials

(i) [7] carried out STXM spectrotomography of PEMFC cathodes at the C and F K-edges, segmenting carbon support from ionomer. (ii) Co/CoO-graphene for the positive electrode of alkaline aqueous batteries was studied at the Co L-edge [8]. (iii) Spectral STXM has been reported of Co-graphene composites, as a model electrocatalyst (work at the Co L-edge and C and O K-edges [9]) or as a system for HER (work at the Co K-edge [11]). (iv) Finally, Ni-N-C composites for CO_2 reduction were mapped by STXM at the Ni L-edge [10].

S2. Literature overview on *ex situ* spectral STXM and spectro-ptychography studies of real-life electrocatalysts

In MnO_2-Ni/NiO-based bifunctional GDEs for Zn-air batteries were studied in pristine and aged conditions by spectral STXM across the Mn L-edge [2, 14]. Moreover, *ex situ* spectro-ptychography at the Ni L-edge has been used for the investigation of Ni-N-C for CO_2 reduction [15] and, in combination with spectral STXM, for the study of Mn-Ni/PPY for bifunctional air electrodes [16].

S3. Literature overview on *in situ* spectral STXM and spectro-ptychography studies of model electrocatalyst materials

First of all, regarding terminology, for clarity, in this paper, our choice is to use the term *in situ* to describe hyperspectal imagining under electrochemical control. This choice is motivated by the fact that the crux of this kind of measurements is to ensure electrochemical control, rather than to acquire data in real time. In any case, the latter experiment would be feasible, if meaningful from the strictly electrochemical viewpoint, in the same wet cell.

As far as STXM work is concerned, following pioneering efforts work in the mid-2010s [6, 8, 17, 18], similar studies have started to appear systematically in the last few years [19-23]. Specifically, *in situ* XRF microscopy and absorption microspectroscopy during electrodeposition was reported of Co-O_x-polypyrrole for oxygen evolution reaction (OER) (work at the Co L-edge: [6, 8]) and of Mn-Co-O_x-polypyrrole for ORR/OER (work at Mn and Co L-edges: [17]). The electrodeposition of the latter electrocatalytic system for reversible oxygen electrodes has also been studied by combined *in situ* XRF microscopy and STXM at Mn and Co L-edges) [18]. More recent studies focussed of *in operando* STXM and absorption microspectroscopy at the Co L-edge of β-$Co(OH)_2$ particles under

OER conditions [19]. *In situ* STXM [21] and spectro-ptychography [20] work has been published of Cu electrodeposition and Cu-catalyzed CO_2 reduction, with measurements at the Cu L-edge and at the C K-edge by combining STXM and ptychography [22]. Moreover, an *in situ* STXM study at the Cu L-edge has been published of Cu electrodeposition and Cu-catalyzed CO_2 reduction, based on a microfluidic wet cell [23]. In addition, *in situ* spectro-ptychography has been employed, either as the only analytic [24] or in combination with STXM, to study MnO_x-polypyrrole electrodeposition for ORR (at Mn L-edge) [24] and CO_2 electroreduction at electrodeposited Cu, with measurements at the Cu L-edge [20, 21] and at C K-edge [22].

S4. Literature overview on *in situ* spectral STXM and spectro-ptychography studies of granular battery materials

[25] first investigated the phase changes of individual $LiFePO_4$ grains by *in situ* STXM at the Fe L-edge. Similar work has been described also in [26] and in [27] where mathematical modelling based in the phase-field approach was employed to follow lithium insertion.

S5. Literature overview on *in situ* differential soft X-ray radiography of electrocatalyst materials

In situ differential soft X-ray radiography, without spectral information, has been employed for the study of electrocatalyst materials. Water formation in real-life Pt/C-based MEAs [28] has been investigated by *in situ* STXM. The electrodeposition/dissolution of Cu_2O particles as candidate materials for CO_2 electroreduction has been described in [29].

S6. Literature overview on *in situ* TEM with close-to-real electrocatalyst materials

Methodology - Strictly methodological work in the field of TEM electrochemical cell development, focused on Ni_xB nanoparticle (NP) immobilization at electron-transparent membranes, has been reported in [30]. The model electrocatalyst was applied by dosing a Ni_xB-ethanol ink with a SECM-monitored pipette. Open-cell electrochemistry is performed to verify the successful deposition of Ni_xB by conducting electrochemical experiments in an electrolyte droplet covering the three-electrode chip. Very weak CV features in system where EtOH dominated the CV pattern were attributed to NiOOH formation from Ni_xB. Moreover, [31] explicitly investigated by TEM the attachment of iron oxide NPs to carbon nanofibers in a wet cell, even though the context is not directly a electrocatalytic one and no electrochemical measurements have been reported. OER - Degradation of Co_3O_4 NPs as model OER electrocatalyst was studies by *in situ* electrochemical TEM in [32]. An ink was formulated with pure NPs suspended in ethanol, that was drop-cast onto an Ar/O_2 plasma sputtered, nanometre-thick carbon adhesion layer evaporated onto the MSES, to improve fixation. The reported CV measurements performed in the cell, exhibit some degree of redox activity of NPs, proving their electrical connection to the WE. Again, regarding OER, [33] visualized *in situ* generation of O_2 bubbles around electrocatalyst Mn_2O_3 NP electrocatalysts. The functional layer was formed by drop-casting an Mn_2O_3-ethanol ink onto an Ar/O_2 plasma etched Si_3N_4 membrane, functionalized with an (unfortunately, highly electrocatalytic) Pt current-collector. Details on electrocatalyst attachment, electrochemical response and possible OER activity towards OER were not reported. CO_2 electroreduction at Cu NPs [34] and nanowires (NWs) [35] was investigated by *in situ* TEM with the aim of identifying active sites and their evolution. The electrodes were prepared by drop-casting particle suspensions in hexane. CV measurements carried out in the TEM cell showed reduction of Cu_2O, thus proving redox activity of drop-cast particles. PEMFC - C-particle supported Pt NPs have been investigated by *in operando* TEM, in view of degradation rationalization [36]. In this study, an ink formulated with commercial electrocatalyst, mixed with Nafion was drop-cast onto the MSES, and the cell was operated in a liquid electrolyte, as model environment. Electrocatalyst attachment and the exact origin of the electrochemical response were not explicitly addressed.

1. Data for Panel B of Figure S2: cyclic voltammetry for bare Au@C TEM grid
Column #1: potential in V; column #2: current in mA
Filename: Fig_S2B_bare.dat

2. Data for Panel B of Figure S2: cyclic voltammetry for a-MnO_2 nanowires transferred to Au@C TEM grid, in air-saturated electrolyte.
Column #1: potential in V; column #2: current in mA
Filename: Fig_S2B_MnO2_air.dat

3. Data for Panel A of Figure 2: cyclic voltammetry for a-MnO_2 nanowires transferred to Au@C TEM grid, in de-aretared electrolyte
Column #1: potential in V; column #2: current in mA
Filename: Fig_2A.dat

4. Data for Panel C of Figure 5: XAS spectrum at the Mn L-edge
Columns #1 and #3: beam energies in eV for the sample and the Mn_2O_3 standard, respectively.
Column #2 XAS signal for the sample.
Column #4 XAS signal for the Mn_2O_3 standard.
XAS signals in arbitrary units.
Filename: Fig_5C.dat

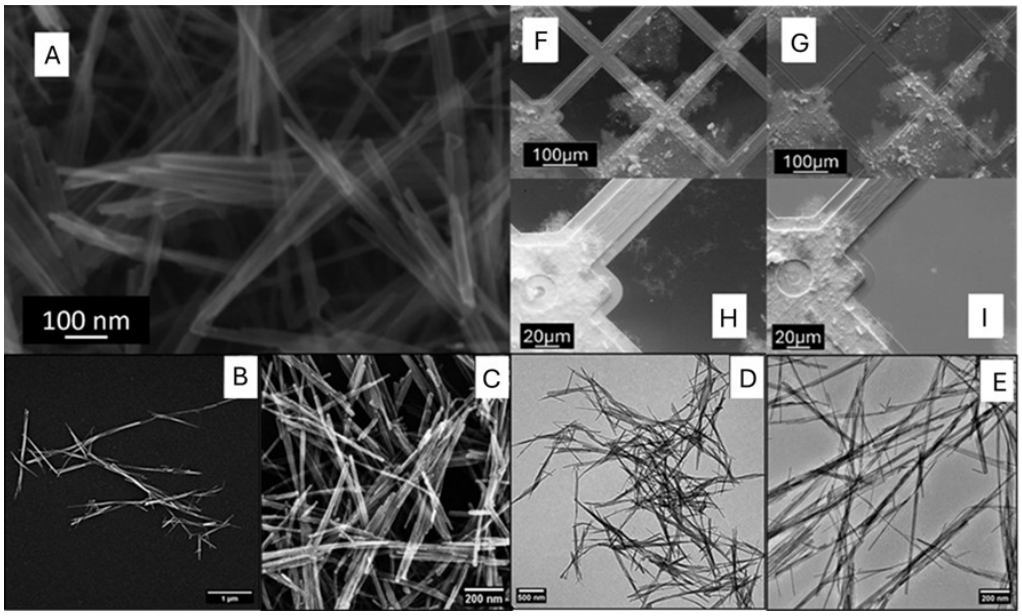

Figure S1 – (A) SEM micrograph and TEM images (B-E) of as-fabricated α-MnO_2 NWs: scale-bar 100 nm. (F- I) The NW-functionalized TEM grid with C coating, in as-deposited state (F, H) and after immersion in 0.1 M KOH (G, I).

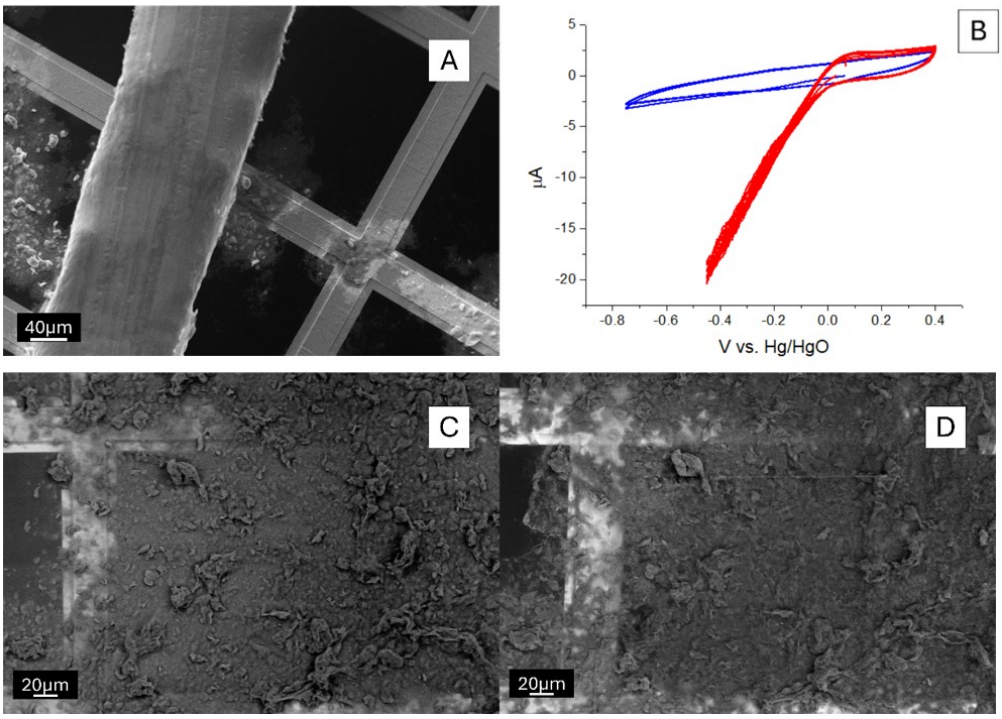

Figure S2 – Functionalized membrane-supported electrode system (FMSES) with Au front-contact. (A) Detail of the NW-functionalized TEM grid with applied mask for front-contact fabrication. (B) Cyclic voltammetry at TEM grid without (blue plot) and with NW-functionalization (red plot) in air-saturated 0.1 M KOH. (C, D) Morphology of the same region of the TEM-grid supported NWs with pinhole-perforated Au overlayer (C) before and after (D) the electrochemical test of (B).

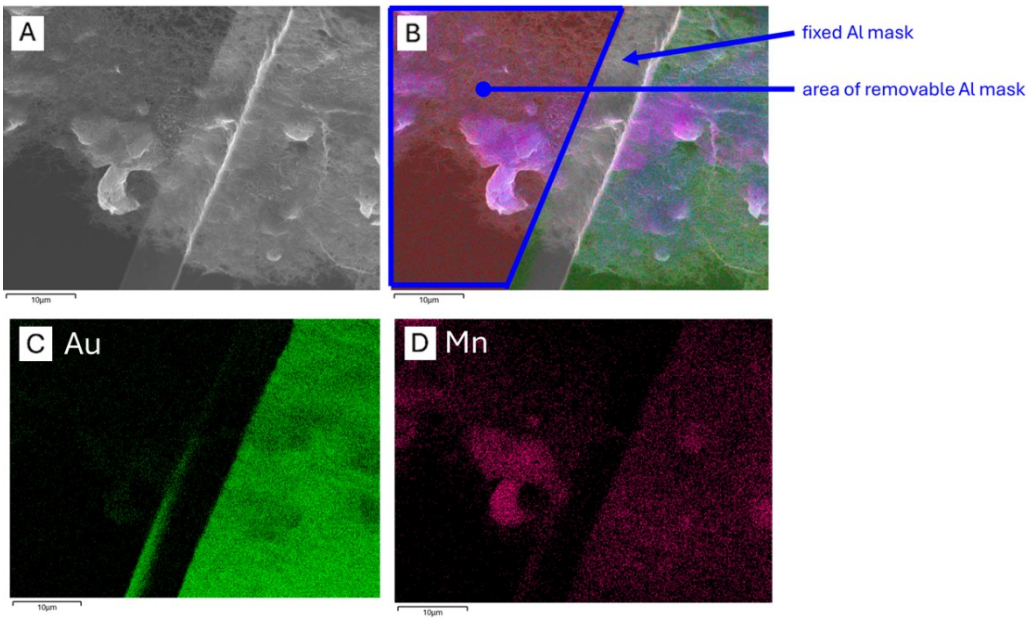

Figure S3 – EDX maps showing the interface between the masked region and the area bearing the Au front-contact, in the functionalized membrane-supported electrode system (FMSES). (A) SEM micrograph. (B) Overlay of SEM image, Au EDX map (green) and Mn EDX map (purple), with indication of the mask positions. (C) Au EDX map. (D) Mn EDX map.